Insights into the nature of plume–asthenosphere interaction from central Pacific geophysical anomalies

Shun-ichiro Karato

Yale University, Department of Geology and Geophysics, New Haven, CT 06520, United States

ARTICLE INFO

ABSTRACT

The central Pacific is one of the type localities where the influence of a plume on the properties of the asthenosphere can be investigated based on the geophysical observations. Recent seismological studies showed enigmatic structures of the upper mantle in the central Pacific. The asthenosphere (~100–200 km depth) in this region has unusually strong $V_{SH}/V_{SV} > 1$ anisotropy associated with relatively weak azimuthal anisotropy. Although less well-constrained, there are suggestions of higher than normal viscosity and lower than normal electrical conductivity in this region. Previous models for the plume–asthenosphere interaction do not easily explain these observations. I propose that these observations are the consequence of a single process: depletion of water by deep partial melting in the plume column. The plume-fed materials in the asthenosphere will be dominated by the olivine A-type fabric whereas in the surrounding normal asthenosphere olivine E-type fabric dominates. This contrast in olivine fabrics provides an explanation for the observed anomalous seismic anisotropy in the central Pacific. Water depletion will also cause high viscosity and low electrical conductivity. The present model implies that plumes supply depleted materials (rather than enriched materials) to the asthenosphere.

© 2008 Elsevier B.V. All rights reserved.

1. Introduction

The OIB (ocean island basalt) and MORB (mid-oceanic ridge basalt) are the two major volcanic rocks on Earth that are believed to be derived from two different regions or components in Earth's mantle. It is generally considered that MORB is derived from "depleted" materials and OIB is from "undepleted" or "enriched" materials (e.g., Zindler and Hart, 1986; Hofmann, 1997; Hofmann, 2004). The way in which these materials (or "reservoirs") interact or mix is one of the main questions in global geodynamics (e.g., Kellogg et al., 1999; Phipps Morgan and Morgan, 1999; Albarède and van der Hilst, 2002; Tackley and Xie, 2002; van Keken et al., 2002; Bercovici and Karato, 2003). In almost all of geodynamic models, materials that produce OIB ("undepleted" or "enriched" regions) are considered to ascend through the upper mantle, and to be added to the asthenosphere that is believed to be the source region of MORB. Consequently, it is important to understand how the injection of plume materials modifies the properties of the asthenosphere. In many models, the plume flux is considered to be so small that the influence of plume materials is negligible (e.g., Davies, 1988; Sleep, 1990). However, there are some hints as to a more important role of plumes affecting the materials' circulation in Earth's mantle (e.g., Phipps Morgan et al., 1995b; Nolet et al., 2006).

The central Pacific is the best place to investigate the nature of plume–asthenosphere interaction because in this area, the Hawaii plume, one of the largest plumes (Sleep, 1990; Montelli et al., 2006), interacts with the Pacific upper mantle that moves with high velocity (relative to the plume). Consequently, a large region of the Pacific upper mantle may show some influence of plume–asthenosphere interaction (e.g., Ribe and Christensen, 1994). In this paper, I will discuss that the reported anomalous properties of the central Pacific asthenosphere including anomalous seismic anisotropy suggest an extensive interaction between plume and ambient asthenospheric materials that causes the asthenosphere in these regions be anomalously depleted with water (hydrogen). I will first review studies reporting various anomalous properties in the asthenosphere of the central Pacific, and then will present a model to explain them based on recent mineral physics and petrological observations. Particularly important in this analysis are the recent finding of the influence of water content on lattice-preferred orientation in olivine (and hence seismic anisotropy) (Jung and Karato, 2001; Karato et al., 2008), the influence of water on viscosity and electrical conductivity of upper mantle minerals (e.g., Mei and Kohlstedt, 2000; Karato, 2006) and the new knowledge on the melting behavior of upper mantle materials (e.g., Hirschmann, 2006).

2. Geophysical anomalies in the central Pacific

There are several geophysical observations or geodynamical inferences that suggest that the asthenosphere in the central Pacific may

have some anomalous properties. Here I review some of these observations or inferences with some notes on the robustness of each result. I will discuss two types of measurements of seismic anisotropy in the central Pacific upper mantle using surface waves: V_{SH}/V_{SV} polarization anisotropy and azimuthal anisotropy. The polarization anisotropy such as V_{SH}/V_{SV} is relatively well-constrained because its measurement is based on the comparison of phase velocities of Rayleigh and Love waves that can be made without large influence of lateral heterogeneity. Ekström and Dziewonski (1998) reported anomalously strong $V_{SH}/V_{SV} > 1$ polarization anisotropy in the central Pacific (surrounding and to the west of Hawaii as well as regions to the south of Hawaii). In this area, the amplitude of V_{SH}/V_{SV} anomaly has a peak in the asthenosphere ~100–150 km and the peak amplitude is about a factor of 2–3 higher than that in other typical oceanic upper mantle. Kustowski et al. (2008) conducted a similar analysis using a more extended data set (Kustowski et al., 2008). The depth variation of the amplitude of polarization anisotropy is markedly different from that in other normal oceanic upper mantle where the amplitude of polarization anisotropy decreases with depth (Montagner and Tanimoto, 1991). A similar result on the V_{SH}/V_{SV} anisotropy was reported by Montagner and Tanimoto (1991), Montagner and Guillot (2000), and by Panning and Romanowicz (2006). The results cited above have much the common features (strong $V_{SH}/V_{SV} > 1$ polarization anisotropy in the asthenosphere) although the magnitude of inferred anisotropy and the exact location differ somewhat among these studies.

The results for azimuthal anisotropy measurements are less robust because the measurements of azimuthal anisotropy involve a comparison of velocities of waves passing through different regions. This causes large uncertainties compared to those in the measurements of polarization anisotropy that involves a comparison on the velocities of Rayleigh and Love waves passing through (nearly) the same paths. Also, azimuthal anisotropy is more sensitive to the details of the structure. Consequently, the results for azimuthal anisotropy show relatively large variations among different studies. In contrast to the strong $V_{SH}/V_{SV} > 1$ polarization anisotropy, Montagner and Tanimoto (1990), Ekström (2000) and Debayle et al. (2005) reported a weak azimuthal anisotropy in the central Pacific compared to the anisotropy near the eastern Pacific rise. As noted above, the observations on the azimuthal anisotropy are less robust than those on the polarization anisotropy and there are some discrepancies in the exact geographical distribution and amplitude of azimuthal anisotropy among different models. For example, weak azimuthal anisotropy is also observed in the south Pacific in some models (Montagner and Tanimoto, 1990; Debayle et al., 2005) (see also Trampert and Woodhouse, 2003; Beucler and Montagner, 2006). Fig. 1 shows some of the seismological observations on anisotropy in the Pacific upper mantle.

In summary, there is strong evidence that the asthenosphere in the central Pacific has unusually strong $V_{SH}/V_{SV} > 1$ anisotropy. Azimuthal anisotropy is less well-constrained but there are observations suggesting relatively weak azimuthal anisotropy in the central Pacific. There are other geophysical observations or inferences that suggest the presence of anomalous properties in the central Pacific. They include anomalously high viscosity and anomalously low electrical conductivity. However, these observations or inferences are less robust than the observations on seismic anisotropy, and I will discuss these observations in the Discussion section.

3. Models for the anomalous seismic anisotropy of the central Pacific

Let us discuss the origin of the most robust feature of the central Pacific anomalies, namely the strong $V_{SH}/V_{SV} > 1$ anisotropy. Since this region corresponds to the region surrounding Hawaii, it is natural to attribute this anomaly to the interaction of Hawaiian plume with the upper mantle (anomalies also extend to the south of Hawaii where smaller hot spots are located). The simplest model for the plume–upper

mantle interaction would be to assume that a plume replaces pre-existing asthenospheric materials with new materials. Phipps Morgan et al. (1995b) proposed such a model to explain average seismic velocities, topography and geoid, but not seismic anisotropy. A simple version of such a model would predict larger shear strains due to larger velocity gradient (and higher temperatures). However, if the larger shear strain was the only consequence of the penetration of a plume into the asthenosphere, it is not obvious how one could explain strong $V_{SH}/V_{SV} > 1$ anisotropy. To understand this problem, let us assume that seismic anisotropy in the upper mantle is due to LPO (lattice-preferred orientation) of olivine (and other minerals) (e.g., Nicolas and Christensen, 1987). Experimental studies have shown that the intensity of LPO increases with strain but approaches a nearly saturated value at a certain strain. This critical strain depends on temperature, water content, etc. but is on the order of ~1–5 (linear shear strain, e.g., (Zhang and Karato, 1995; Bystricky et al., 2001; Jung et al., 2006); critical strain is lower at higher temperature and high water content and the lower end of critical strain is likely the plausible value for the asthenosphere). Shear strain in the asthenospheric material would be ~15–30 when they have moved from the east Pacific rise to Hawaii assuming the passive shear deformation in a 100–200 km thick layer by the surface plate motion of ~3000 km. Therefore LPO should have been saturated in most of the oceanic asthenosphere and it is unlikely that any strong shear flow near Hawaii increases the strength of LPO.

What mechanisms could enhance V_{SH}/V_{SV} polarization anisotropy if the intensity of LPO is saturated? One mechanism is the change in the fabric type of olivine due to the change in water content. Recently Jung and Karato (2001) and Katayama et al. (2004) (see also a review by Karato et al., 2008) showed that water content has an important effect on olivine deformation fabrics (LPO). When olivine is deformed under a high water content (and low stress) condition, it will assume the C-type fabric (for the definitions of various fabric types, see Karato et al., 2008). At a modest water content (and a low stress), the E-type fabric will be dominant. However, when olivine is deformed under water-poor conditions, a different fabric, the A-type fabric will dominate. In most of the lithosphere, olivine A-type is expected to dominate based on the laboratory studies that are consistent with the observations on a large number of naturally deformed peridotites (e.g., Nicolas and Christensen, 1987; Ben Ismail and Mainprice, 1998).

Let us consider what may happen when a plume material ascends through the upper mantle asthenosphere where ambient olivine assumes the E-type fabric. The petrological studies suggest that the melting in a plume occurs at ~150–200 km as opposed to ~60 km beneath the mid-ocean ridges because of the higher temperatures (and a higher water content) (Hirschmann, 2006). After partial melting, a large fraction of water (hydrogen) is removed from the solid minerals to the melt that is carried rapidly to the surface without much diffusion. Consequently, much of the solid materials in a plume column above this depth will be composed of depleted (water-poor) materials, although the original plume materials are water-rich compared to the materials in the typical upper mantle (Wallace, 1998). Therefore plume materials likely have olivine C-type fabric in the deep upper mantle, but the regions of the asthenosphere that have been replaced with plume materials after partial melting will produce olivine A-type fabric (Karato et al., 2008). Therefore a plausible model for the distribution of olivine fabrics is that the ambient asthenosphere has the E-type fabric, whereas the plume-affected asthenosphere will have the A-type fabric. Different olivine fabrics show different types of seismic anisotropy. In olivine the elastic stiffness is the largest for deformation along the [100]-axis and the least along the [010]-axis. Consequently, for the A-type fabric where the olivine [010]-axis is in the vertical direction (for the horizontal shear; see Fig. 2), we expect strong $V_{SH}/V_{SV} > 1$ anisotropy and weak azimuthal anisotropy. In contrast, for the olivine E-type fabric where the olivine [001]-axis is in the vertical direction (for the horizontal shear; see Fig. 2), we expect weak $V_{SH}/V_{SV} > 1$ anisotropy and strong azimuthal anisotropy. I have calculated the amplitude of V_{SH}/V_{SV} anisotropy (assuming
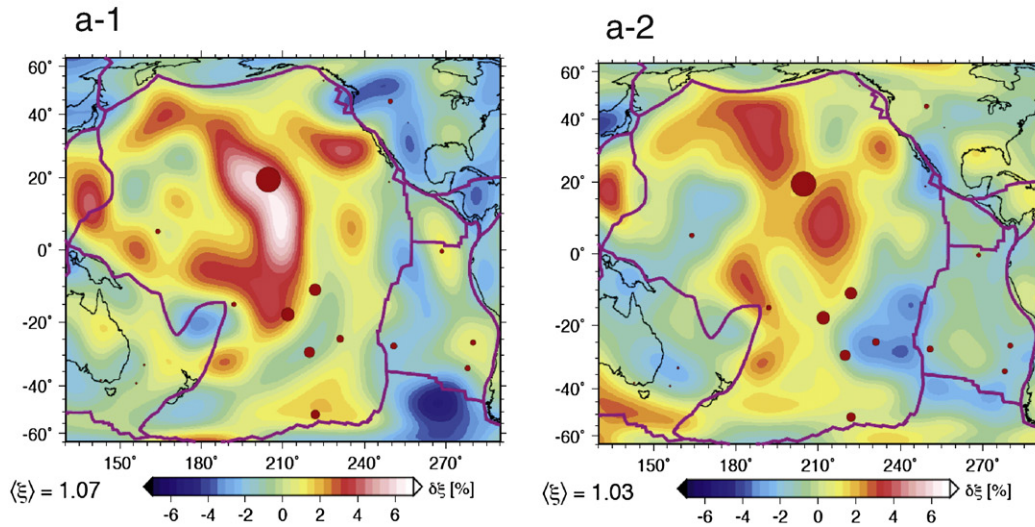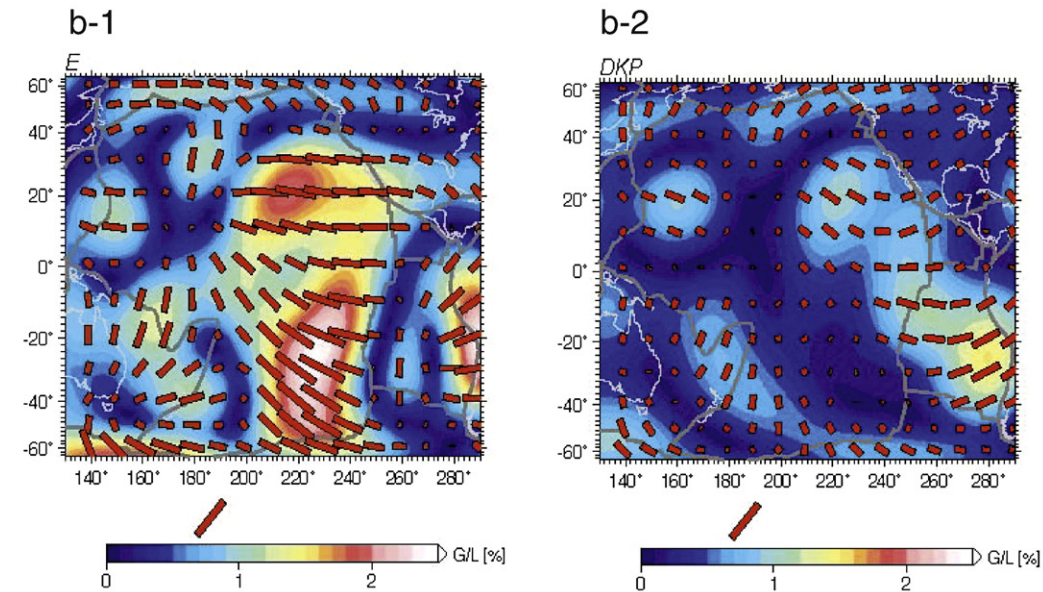
Fig. 1. (a) The V_{SH}/V_{SV} anisotropy in the Pacific at ~150 km depth (asthenosphere) (a-1): from Kustowski et al. (2008), and (a-2) from Panning and Romanowicz (2006). (b) The azimuthal anisotropy in the Pacific at ~150 km depth. The bars show the directions of the fast Rayleigh wave and the length indicates its strength. The strength of azimuthal anisotropy is also shown by G/L that is proportional to the square of the azimuthal anisotropy of $\cos 2\psi$ term (ψ: azimuth of propagation of the waves) (e.g., Montagner and Nataf, 1986) (b-1) from Ekström (2000), and (b-2) from Debayle et al. (2005). The red dots indicate the position of hot spots.

transverse isotropy) as well as the azimuthal anisotropy of the SV and P waves corresponding to the horizontal shear based on the calculated elastic constants of olivine aggregates from the measured orientation distribution function. The results are summarized in Fig. 2 that shows the contrasting characteristics of the olivine A- and E-type fabrics (for more details of the data see Appendix). The olivine A-type fabric causes strong $V_{SH}/V_{SV} > 1$ anisotropy whereas it causes weak azimuthal anisotropy. In contrast, the olivine E-type fabric causes weak $V_{SH}/V_{SV} > 1$ anisotropy and strong azimuthal anisotropy (the difference is more marked for V_{SH}/V_{SV} anisotropy than for azimuthal anisotropy). In the typical oceanic upper mantle, the lithosphere will have the olivine A-type fabric while the asthenosphere will have the E-type fabric which results in decreasing amplitude of $V_{SH}/V_{SV} > 1$ anisotropy with depth associated with increasing amplitude of azimuthal anisotropy with

depth. These features are consistent with the known general features of typical oceanic upper mantle (Montagner and Tanimoto, 1990; Montagner and Tanimoto, 1991; Trampert and van Heijst, 2002; Debayle et al., 2005). However, when a plume replaces the pre-existing materials (with modest water content) with water-poor materials then the asthenosphere materials in that region will have the olivine A-type fabric rather than the E-type fabric. Then the asthenosphere in that region will have strong $V_{SH}/V_{SV} > 1$ anisotropy associated with weak azimuthal anisotropy when the flow geometry is horizontal. These are exactly the nature of anomalies in seismic anisotropy reported for the central Pacific. The regions of the asthenosphere affected by theses plume-fed materials will extend from the plume location drifted to some extent to the west due to the interaction of the plate motion (Ribe and Christensen, 1994) (see Fig. 3).

4. Discussion

Are there any other models to explain the observed geophysical anomalies in the central Pacific? I have already discussed that if only larger shear strain associated with a plume is considered, then it is difficult to explain the strong polarization anisotropy because the strength of deformation fabric should be saturated in the central Pacific without the influence of a plume. Also, it is not clear how the larger shear strain could cause weak azimuthal anisotropy. I note that the observed weak azimuthal anisotropy could be attributed to the modification of the orientation of olivine [100]-axis by the modification of radial flow pattern due to Hawaiian plume, but if the orientation of olivine [100] is controlled partly by the plate motion and partly by the plume, it is not clear if both the strong $V_{SH}/V_{SV} > 1$ anisotropy and weak azimuthal anisotropy are explained in a consistent way. In addition, such a model would imply that the electrical conductivity in the asthenosphere of the central Pacific is higher than normal and the viscosity is lower than normal, which is not consistent with the observations as will be discussed later.

Another frequently invoked cause for anomalies in seismic anisotropy in the old asthenosphere is the influence of small-scale convection (e.g., Montagner, 2002). There are some observations suggesting the presence of small-scale convection in the old asthenosphere (e.g., Haxby and Weissel, 1986), but its influence on seismic anisotropy is not well understood. In particular, it is not clear how small-scale convection can increase the magnitude of polarization anisotropy. Using a simple model, one would expect that small-scale convection will reduce the long wave-length anisotropy particularly the polarization anisotropy because material motion associated with
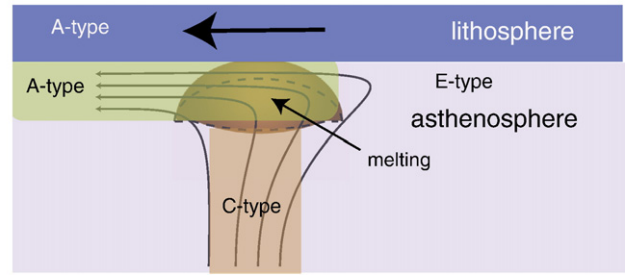

Fig. 3. A model of melting and water re-distribution in the plume column in the upper mantle. Significant melting in a plume column occurs in the deep upper mantle (~150–200 km) when the temperature exceeds the dry solidus, and hence when the plume materials change flow direction from vertical to horizontal above ~200 km depth (Ribe and Christensen, 1994), majority of materials fed by a plume to the shallow asthenosphere will be depleted ("dry") materials.

small-scale convection includes both vertical and horizontal shear. Therefore the onset of small-scale convection might explain weak azimuthal anisotropy but not the strong polarization anisotropy. In fact, Montagner (2002) suggested that the observed weak anisotropy in some regions in the old Pacific might be caused by small-scale convection.

Recently, Becker et al. (2008) proposed a model to explain the strong $V_{SH}/V_{SV} > 1$ anisotropy through global convection modeling. In their model, the strong $V_{SH}/V_{SV} > 1$ anisotropy is correlated to strong shear flow (see their Figs. 3 and 5c). Although they also considered the influence of water, the relation between water content and seismic anisotropy is not clearly demonstrated in their model, and the
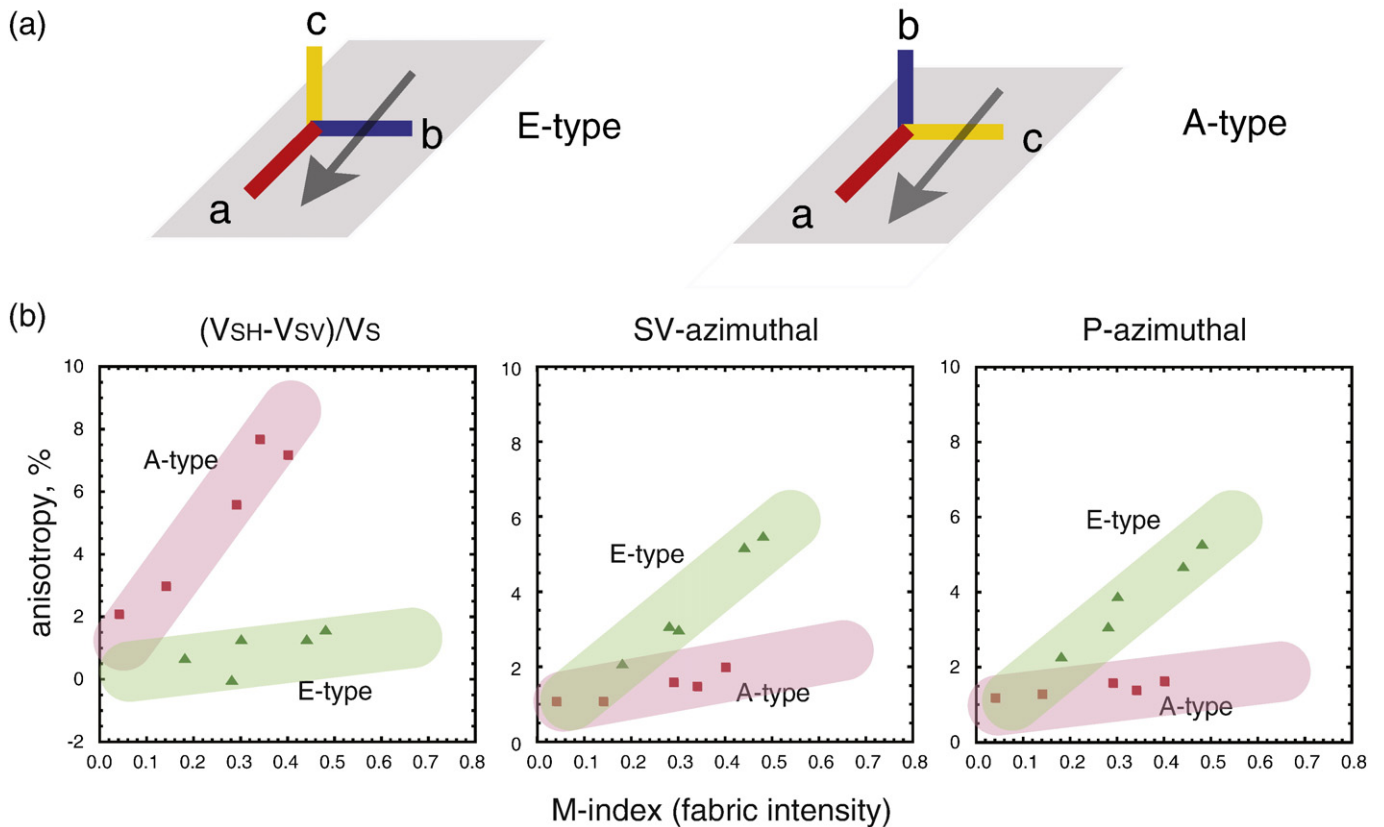

Fig. 2. Seismic anisotropy for two different fabric types of olivine. (a) Schematic diagrams showing the orientations of olivine crystallographic axes in the shear flow. (b) The amplitude of the $V_{SH}/V_{SV}((V_{SH} - V_{SV})/V_S)$ anisotropy and azimuthal anisotropy of SV and P waves for different olivine fabrics corresponding to the horizontal flow as a function of M-index (an indicator of fabric strength: M-index is 0 for a random LPO, and is 1 for a perfect LPO (Skemer et al., 2005)). Azimuthal anisotropy of Rayleigh waves reflects that of SV and P waves. For the same strength of fabric (M-index), A-type fabric produces much stronger V_{SH}/V_{SV} anisotropy and somewhat weaker azimuthal anisotropy than E-type fabric (for C-type fabric, $V_{SH}/V_{SV} < 1$ (not shown)). The data used include those from experimental studies (Jung et al., 2006) and from naturally deformed peridotites (see Appendix). Typical values of M-index for naturally deformed peridotites (mostly from the lithosphere) are 0.2 to 0.4 (Skemer et al., 2005).

strongest factor to control the distribution of (radial) anisotropy is the larger shear strains associated with a plume.

In fact, the inferred water distribution (shown in their Fig. 7) in the Pacific is opposite to a model that I propose in this paper based on mineral physics. As discussed earlier, the correlation between strong shear and strong anisotropy seen in their model is not consistent with the laboratory data showing a small saturation strain for LPO evolution.

There have been a few geodynamic modeling to constrain the viscosity of the asthenosphere beneath the Hawaiian swell (e.g., Watson and McKenzie, 1991; Phipps Morgan et al., 1995a). In these studies, the viscosity of the asthenosphere is inferred from geodynamic modeling of the support of topography associated with the Hawaiian plume. These studies suggested viscosity values of ~ 3× 10^{19} Pa s(Watson and McKenzie, 1991) or ~ 2 × 10^{20} Pa s (Phipps Morgan et al., 1995a). These values are substantially larger than the viscosity of a typical oceanic asthenosphere (~ 10^{18} Pa s: e.g., Davaille and Jaupart, 1994; Pollitz et al., 1998). In fact Phipps Morgan et al. (1995a) suggested that the high viscosity of the asthenosphere there might be due to the removal of water from the asthenosphere by partial melting.

Now let me provide some evidence suggesting that the central Pacific is also anomalous in terms of electrical conductivity. Inferring the electrical conductivity from geomagnetic induction is more complicated due largely to the effects of highly conductive oceans and the limitation of the frequency range of the data (e.g., Heinson and Constable, 1992). Therefore the lateral and depth variation in electrical conductivity cannot be inferred as convincingly as that of seismic anisotropy. Nevertheless, some trends can be inferred. For example, the upper mantle conductivity inferred for the eastern Pacific (Lizarrale et al., 1995) is considerably higher than that for a majority of the Pacific (Utada et al., 2003), suggesting that the central Pacific has a significantly lower conductivity than in the eastern Pacific. Similarly, a systematic difference in conductivity between the eastern and the central Pacific regions is found by Heinson and Constable (1992) and Oldenburg (1981). Fig. 4 summarizes the reported electrical conductivity profiles in the upper mantle in various regions of the Pacific and the surrounding areas together with the calculated

conductivity profiles corresponding to various water contents (I assumed a geotherm corresponding to 60 My old, if other ages were used the inflection point will move its depth but the conductivity values at the deeper part will not be affected). We find that the conductivity profiles in the eastern Pacific can be explained by a water content of ~0.01 wt.%, whereas the conductivity in the central Pacific corresponds to almost water-free (dry) olivine. It should be noted that although the models by Utada et al. (2003) are called a semi-global model, the majority of the data are from the central Pacific. Therefore I conclude that the electrical conductivity in the asthenosphere in the central Pacific is significantly lower than those in other regions.

In summary, although not well-constrained, the observations or inferences of viscosity and electrical conductivity in the central Pacific region provide additional support for the present model, but these observations are not consistent with a simple model of enhanced flow by a hot plume that would predict the opposite.

Is this model consistent with the inferred mass flux for the Hawaiian plume? The buoyancy flux of the Hawaiian plume is estimated to be ~9×10^3 kg/s (Sleep, 1990), which corresponds to a mass flux of ~1.5×10^6 kg/s assuming ~200 K of the excess temperature. If I assume that the pre-existing asthenosphere materials replaced by the depleted plume materials have been moving with the same velocity as the overlying plate, then the duration of feeding of the depleted materials currently in the central/western Pacific is ~80 My. This yields ~4×10^{21} kg or ~1.3×10^9 km^3. The volume of anomalous asthenosphere may also be estimated from the region of anomalous V_{SH}/V_{SV} anisotropy (Ekström and Dziewonski, 1998; Ekström, 2000) to be ~1–2×10^9 km^3 from seismological observations. The agreement is satisfactory considering the large uncertainties (a factor of ~2) in these estimates.

5. Concluding remarks

I have shown that the anomalously strong $V_{SH}/V_{SV}>1$ associated with weak azimuthal anisotropy, high viscosity and low electrical conductivity in the asthenosphere of the central Pacific can be attributed to a single common cause: a lower water content than in the typical asthenosphere. This model provides a unified explanation for several geophysical anomalies in the central Pacific and suggests that plumes could have an important influence on the (trace element) compositions of the asthenosphere. Interestingly, this model suggests that the presence of less depleted basalt (OIB) on the surface has a highly depleted counterpart at depths (i.e., asthenosphere) as a result of partial melting and resultant material segregation. This is analogous to the structure of the continental region as proposed by Jordan (1975) (Jordan, 1975). Together with the influence of subducted paleo-oceanic crust (e.g., Hirschmann and Stolper, 1996), the interaction between plumes and the asthenosphere could cause regional variation in the trace element composition in the upper mantle.

However, many of the geophysical observations that I cited are not quite robust. In particular, the spatial distribution of seismic anisotropy is not very well-constrained particularly for the azimuthal anisotropy, and the inference of lateral variation of electrical conductivity is based on a sketchy data set. The present model can be examined more definitively if improved geophysical observations become available. For example, this model predicts that there could be a change in seismic wave velocities in a plume column at ~150–200 km depth where a significant partial melting occurs (exact depth depends on plume temperature and water content). Such a change could be detected by high-resolution seismological studies. Also, the model predicts a low electrical conductivity in the central (or the western to central) Pacific. Currently no reliable observations are available to test the regional variation in electrical conductivity in the Pacific. These improved geophysical measurements together with improved mineral physics studies will provide new insights into the interaction between a plume and the upper mantle.
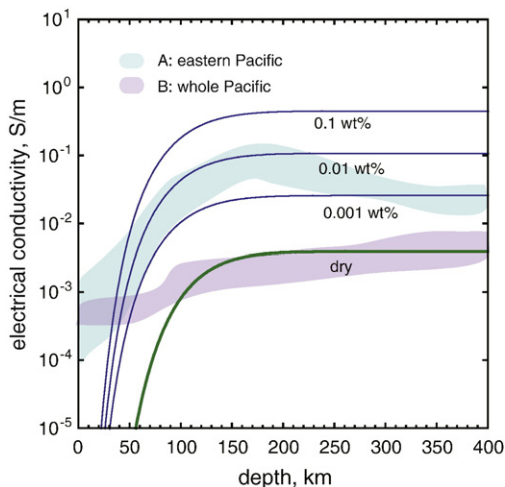

Fig. 4. Electrical conductivity in the upper mantle and the conductivity–depth profiles corresponding to various water contents. A: eastern Pacific (Lizarrale et al., 1995), B: whole Pacific (Utada et al., 2003). The results for the whole Pacific are dominated by the data from the central Pacific and largely represent the conductivity profile of the central Pacific. The conductivity-profiles corresponding to various water contents are calculated based on the data by Wang et al. (2006) and a standard oceanic geotherm for 60 My old oceanic upper mantle. The results show that although the results from the asthenosphere of the eastern Pacific and Philippine Sea regions can be explained by a typical water content of ~0.01 wt.% (Hirschmann, 2006), the results for the whole (central) Pacific suggest water-poor asthenosphere.

Acknowledgments

Appendix A: Seismic anisotropy and deformation fabrics

For a given deformation fabric, a rock has a certain type of elastic (seismic) anisotropy. Anisotropy has its geometry and strength. The geometry of anisotropy is unique to the type of deformation fabrics (A-type, E-type etc.), and for a given fabric type the intensity of anisotropy increases with the increase in the strength of fabrics. Skemer et al. (2005) introduced a new measure of intensity of deformation fabrics ("M-index"), and showed that there is a good correlation between the magnitude of seismic anisotropy and the M-index for a given fabric type. However such a trend depends on the fabric type: for different fabric type, a different trend is present. In particular, because of the difference in the geometry of the fabrics, the A-type and E-type fabrics show distinct strength for azimuthal anisotropy and V_{SH}/V_{SV} anisotropy.

Actual calculations were based on the following eleven samples listed in Table 1, and the results shown in Fig. 2 were made only for olivine. The elastic constants of each sample were calculated using the Voigt–Reuss–Hill average scheme. Seismic anisotropy was calculated from the calculated elastic constants using a method by Montagner and Nataf (1986) that applies to a weakly anisotropic material. The elastic constants of olivine at 5 GPa and 1573 K were used. To the extent that such a diagram as Fig. 2 shows the variation in strength of a fabric with the fabric intensity (M-index) for a given fabric type, the choice of samples has only minor influence. The more important limitation is the ignorance of other minerals such as orthopyroxene. The influence of orthopyroxene and other minerals cannot be included in any detail in such a study because there is no experimental data on the influence of water on deformation fabrics of orthopyroxene. The limited observations on naturally deformed peridotites suggest that the deformation fabrics of orthopyroxene do not change with water content so much (see Karato et al., 2008) but obviously much more detailed studies are required to address this issue. Also the results summarized in Table 1 show that at least for the A-type fabric, the influence of orthopyroxene is minor.

References

Albarède, F., van der Hilst, R.D., 2002. Zoned mantle convection. Phil. Trans. Royal. Soc. London. **A360**, 2569–2592.
Becker, T.W., Kustowski, B., Ekström, G., 2008. Radial seismic anisotropy as a constraint for upper mantle rheology. Earth and Planetary Science Letters **267**, 213–227.
Ben Ismail, W., Mainprice, D., 1998. An olivine fabric database: an overview of upper mantle fabrics and seismic anisotropy. Tectonophysics **296**, 145–157.
Bercovici, D., Karato, S., 2003. Whole mantle convection and transition-zone water filter. Nature **425**, 39–44.
Beucler, E., Montagner, J.-P., 2006. Computation of large anisotropic seismic heterogeneities (CLASH). Geophys. J. Int. **165**, 447–468.
Bystricky, M., Kunze, K., Burlini, L., Burg, J.-P., 2001. High shear strain of olivine aggregates: rheological and seismic consequences. Science **290**, 1564–1567.
Davaille, A., Jaupart, C., 1994. Onset of thermal convection in fluids with temperature-dependent viscosity: application to the oceanic mantle. J. Geophys. Res. **99**, 19853–19866.
Davies, G.F., 1988. Ocean bathymetry and mantle convection, 1. Large-scale flows and hotspots. J. Geophys. Res. **93**, 10,467–10,480.
Debayle, E., Kennett, B.L.N., Priestley, K., 2005. Global azimuthal seismic anisotropy and the unique plate-motion deformation of Australia. Nature **433**, 509–512.
Ekström, G., 2000. Mapping the lithosphere and asthenosphere with surface waves: lateral structure and anisotropy. In: Richards, M.A., Gordon, R.G., Hilst, R. v. d. (Eds.), The History and Dynamics of Global Plate Motions. American Geophysical Union, pp. 239–255.
Ekström, G., Dziewonski, A.M., 1998. The unique anisotropy of the Pacific upper mantle. Nature **394**, 168–172.
Haxby, W., Weissel, J., 1986. Evidence for small-scale convection from SEASAT altimetry data. J. Geophys. Res. **91**, 3507–3520.
Heinson, G., Constable, S., 1992. The electrical conductivity of the oceanic upper mantle. Geophys. J. Int. **110**, 159–179.
Hirschmann, M.M., 2006. Water, melting, and the deep Earth H_2O cycle. Ann. Rev. Earth. Planet. Sci. **34**, 629–653.
Hirschmann, M.M., Stolper, E.M., 1996. A possible role for garnet pyroxenite in the origin of the "garnet signature" in MORB. Contrib. Miner. Petrol. **124**, 185–208.
Hofmann, A.W., 1997. Mantle geochemistry: the message from oceanic volcanism. Nature **385**, 219–228.
Hofmann, A.W., 2004. Sampling mantle heterogeneity through oceanic basalts: isotopes and trace elements. In: Holland, H.D., Turekian, K.K. (Eds.), Treatise on Geochemistry, vol. v.2. Elsevier, pp. 61–101.
Jordan, T.H., 1975. The continental tectosphere. Rev. Geophys. Space. Phys. **13**, 1–12.
Jung, H., Karato, S., 2001. Water-induced fabric transitions in olivine. Science **293**, 1460–1463.
Jung, H., Katayama, I., Jiang, Z., Hiraga, T., Karato, S., 2006. Effects of water and stress on the lattice preferred orientation in olivine. Tectonophysics **421**, 1–22.
Karato, S., 2006. Influence of hydrogen-related defects on the electrical conductivity and plastic deformation of mantle minerals: a critical review. In: Jacobsen, S.D., van der Lee, S. (Eds.), Earth's Deep Water Cycle. American Geophysical Union, pp. 113–129.
Karato, S., Jung, H., Katayama, I., Skemer, P.A., 2008. Geodynamic significance of seismic anisotropy of the upper mantle: new insights from laboratory studies. Ann. Rev. Earth. Planet. Sci. **36**, 59–95.
Katayama, I., Jung, H., Karato, S., 2004. New type of olivine fabric at modest water content and low stress. Geology **32**, 1045–1048.
Kellogg, L.H., Hager, B.H., van der Hilst, R.D., 1999. Compositional stratification in the deep mantle. Science **283**, 1881–1884.
Kustowski, B., Ekström, G., Dziewonski, A.M., 2008. Anisotropic shear-wave velocity structure of the Earth's mantle: a global model. J. Geophys. Res. **113**. doi:10.1029/2007JB005169.
Lizarralde, D., Chave, A., Hirth, G., Schultz, A., 1995. Northeastern Pacific mantle conductivity profile from long-period magnetotelluric sounding using Hawaii-to-California cable data. J. Geophys. Res. **100**, 17837–17854.
Mehl, L., Hacker, B.R., Hirth, G., Kelemen, P.B., 2003. Arc-parallel flow within the mantle wedge: evidence from the accreted Talkeetna arc, south central Alaska. J. Geophys. Res. **108**. doi:10.1029/2002JB002233.
Mei, S., Kohlstedt, D.L., 2000. Influence of water on plastic deformation of olivine aggregates, 2. Dislocation. creep. regime. J. Geophys. Res. **105**, 21471–21481.
Montagner, J.-P., 2002. Upper mantle low anisotropy channels below the Pacific Plate. Earth. Planet. Sci. Lett. **202**, 263–274.
Montagner, J.-P., Nataf, H.-C., 1986. A simple method for inverting the azimuthal anisotropy of surface waves. J. Geophys. Res. **91**, 511–520.

Table 1
Samples used in Fig. 2

Sample	M-index	Azimuthal (SV) (%)	Azimuthal (P) (%)	$(V_{SH}-V_{SV})/V_S$ (%)
A-type				
(1)	0.04	1.1	1.2	2.1
(2)	0.14	1.1	1.3	3.0
(3)	0.29	1.6	1.7	5.6
(4)	0.34	1.5	1.4	7.7
(5)	0.40	2.0	1.6	7.2
(6)	–	1.6	2.3	5.7
E-type				
(7)	0.18	2.1	2.3	0.7
(8)	0.28	3.1	3.1	0.0
(9)	0.30	3.0	3.9	1.3
(10)	0.44	5.2	4.7	1.3
(11)	0.48	5.5	5.3	1.6

(1): A sample deformed in the lab at P=0.3 GPa, T=1573 K, less than 100 ppm H/Si.
(2): A sample deformed in the lab at P=0.3 GPa, T=1573 K, less than 100 ppm H/Si.
(3), (4), (5): Sheared lherzolites from South Africa (samples donated by Joe Boyd). Only olivine is included in these calculations.
(6): Based on the elastic constants for a harzburgite (74% olivine, 22% orthopyroxene, 4% other minerals (Peselnick and Nicolas, 1978)) including contributions from all minerals. Because the M-index is not available for this sample, the results from this sample are not included in Fig. 1. However, this sample indicates that the trend in seismic anisotropy for this sample is similar to those for pure olivine. I conclude that the influence of orthopyroxene on seismic anisotropy is not very strong.
(7): A sample deformed in the lab at P=2 GPa, T=1470 K, 210 ppm H/Si.
(8): A sample deformed in the lab at P=2 GPa, T=1470 K, 560 ppm H/Si.
(9): A sample deformed in the lab at P=2 GPa, T=1470 K, 630 ppm H/Si.
(10): A sample deformed in the lab at P=2 GPa, T=1470 K, 280 ppm H/Si.
(11): A harzburgite from Talkeetna arc, Alaska (Mehl et al., 2003). Only olivine is included in this calculation.

Montagner, J.-P., Tanimoto, T., 1990. Global anisotropy in the upper mantle inferred from the regionalization of phase velocities. J. Geophys. Res. **95**, 4797–4819.

Montagner, J.-P., Tanimoto, T., 1991. Global upper mantle tomography of seismic wave velocities and anisotropies. J. Geophys. Res. **96**, 20337–20351.

Montagner, J.P., Guillot, L., 2000. Seismic anisotropy in the Earth's mantle. In: Boschi, E., Ekström, G., Morelli, A. (Eds.), Problems in Geophysics for the New Millenium, pp. 217–253 (Editrice Compositori).

Montelli, R., Nolet, G., Dahlen, F.A., Masters, G., 2006. A catalogue of deep mantle plumes: new results from finite-frequency tomography. Geochem. Geophys. Geosyst. **7 (11)**. doi:10.1029/2006GC001248.

Nicolas, A., Christensen, N.I., 1987. Formation of anisotropy in upper mantle peridotite: a review. In: Fuchs, K., Froidevaux, C. (Eds.), Composition, Structure and Dynamics of the Lithosphere–Asthenosphere System. American Geophysical Union, pp. 111–123.

Nolet, G., Karato, S., Montelli, R., 2006. Plume fluxes from seismic tomography: a Bayesian approach. Earth. Planet. Sci. Lett. **248**, 685–699.

Oldenburg, D.W., 1981. Conductivity structure of oceanic upper mantle beneath the Pacific plate. Geophysical Journal of the Royal Astronomical Society **65**, 359–394.

Panning, M., Romanowicz, B., 2006. A three-dimensional radially anisotropic model of shear velocity in the whole mantle. Geophys. J. Int. **167**, 361–379.

Peselnick, L., Nicolas, A., 1978. Seismic anisotropy in an ophiolite peridotite: application to oceanic upper mantle. J. Geophys. Res. **83**, 1227–1235.

Phipps Morgan, J., Morgan, J.W., 1999. Two-stage melting and the geochemical evolution of the mantle: a recipe for mantle plum-pudding. Earth. Planet. Sci. Lett. **170**, 215–239.

Phipps Morgan, J., Morgan, J.W., Price, E., 1995a. Hotspot melting generates both hotspot volcanism and a hotspot swell? J. Geophys. Res. **100**, 8045–8062.

Phipps Morgan, J., Morgan, W.J., Zhang, Y.-S., Smith, W.H.F., 1995b. Observational hints for a plume-fed, suboceanic asthenosphere and its role in mantle convection. J. Geophys. Res. **100**, 12753–12767.

Pollitz, F.F., Brgmann, R., Romanowicz, B., 1998. Viscosity of oceanic asthenosphere inferred from remote triggering of earthquakes. Science **280**, 1245–1249.

Ribe, N.M., Christensen, U.R., 1994. Three-dimensional modeling of plume–lithosphere interaction. J. Geophys. Res. **99**, 669–682.

Skemer, P.A., Katayama, I., Jiang, Z., Karato, S., 2005. The misorientation index: development of a new method for calculating the strength of lattice-preferred orientation. Tectonophysics **411**, 157–167.

Sleep, N.H., 1990. Hotspots and mantle plumes: some phenomenology. J. Geophys. Res. **95**, 6715–6736.

Tackley, P.J., Xie, S.X., 2002. The thermochemical structure and evolution of Earth's mantle: constraints and numerical models. Phil. Trans. Royal. Soc. London. **360**, 2593–2609.

Trampert, J., van Heijst, H.J., 2002. Global azimuthal anisotropy in the transition zone. Science **296**, 1297–1299.

Trampert, J., Woodhouse, J.H., 2003. Global anisotropic phase velocity maps for fundamental mode surface waves between 40 and 150 seconds. Geophys. J. Int. **154**, 154–165.

Utada, H., Koyama, T., Shimizu, H., Chave, A.D., 2003. A semi-global reference model for electrical conductivity in the mid-mantle beneath the north Pacific region. Geophys. Res. Lett. **30**. doi:10.1029/2002GL016092.

van Keken, P.E., Hauri, E.H., Ballentine, C.J., 2002. Mantle mixing: the generation, preservation, and destruction of chemical heterogeneity. Ann. Rev. Earth. Planet. Sci. **30**, 493–525.

Wallace, P., 1998. Water and partial melting in mantle plumes: inferences from the dissolved H_2O concentrations of Hawaii basaltic magmas. Geophys. Res. Lett. **25**, 3639–3642.

Wang, D., Mookherjee, M., Xu, Y., Karato, S., 2006. The effect of water on the electrical conductivity in olivine. Nature **443**, 977–980.

Watson, S., McKenzie, D., 1991. Melt generation by plumes: a study of Hawaiian volcanism. J. Petrol. **32**, 501–537.

Zhang, S., Karato, S., 1995. Lattice preferred orientation of olivine aggregates deformed in simple shear. Nature **375**, 774–777.

Zindler, A., Hart, S., 1986. Chemical geodynamics. Ann. Rev. Earth. Planet. Sci. **14**, 493–570.